

Article

Comparative Study of Frequency Converters for Doubly Fed Induction Machines

Tarek Nahdi and Dusan Maga *

Czech Technical University in Prague, 166 36 Prague, Czech Republic; tareknah@fel.cvut.cz

* Correspondence: dusan.maga@fel.cvut.cz; Tel.: +420-224-354-021

Received: 21 January 2018; Accepted: 22 February 2018; Published: 26 February 2018

Abstract: The efficient utilization of energy sources seems to be one of the most challenging problems for designers and scientists alike. This challenge particularly applies to power electronics, where the increasing value of energy density leads to demands for optimization processes and better exploitation (and distribution) of available power sources. As a result, the implementation of frequency-controlled systems is more often in the spotlight. The systems with doubly fed induction machines and a frequency converter in the rotor circuit are typical representatives of these demands. In a wide spectrum of power electronic systems, frequency converters are often used that have a constant current, a diode rectifier, and a thyristor inverter. This article provides a novel approach to modeling methodology, and presents a unique comparison of four different frequency converter schemes that are connected to a doubly fed induction machine. This article presents the modeling methodology itself, as well as the results based on an asynchronous generator motor fed by different frequency converters, a spectral analysis of the output voltage of the used frequency converters, and a comparison of the different technologies. Based on the above, this paper recommends the use of a multistage-multilevel frequency converter scheme.

Keywords: doubly-fed induction machines; frequency converter; output voltage spectral analysis

1. Introduction

Many authors have addressed the problems related to frequency converters (FCs) in recent years. However, only few of them have focused on doubly fed induction machines (DFIM). We consider especially Pronin et al. [1], where authors pay attention to the composition of FC–DFIM system electrical units; their work also contains a detailed description of a DFIM scheme and a mathematical expression of its properties, which is necessary for its computer modeling. The paper can be considered a fundamental step towards presented simulations and procedures that are applied to the same technology and used in the same industrial company.

In Steimer et al. [2], we find a rare example from independent authors with a similar research focus and a clear link to industrial application. Although their primary area of interest consists of converter-fed machines for pumped hydro storage plants, nevertheless, the authors replaced a DFIM machine with a synchronous one (with reference to an installation in Switzerland from 2013). Therefore, the paper logically addresses converter-fed synchronous machine (CFSM) technology, including the differences between CFSM and DFIM. Generally, the technology is intended for an environment that is characterized by rapid changes of the residual load (such as unavoidable consequences of wind and solar power sources).

Also in Cuesta et al. [3], there is a clear link to practical applications. The authors use a FC in connection with a classical (squirrel cage) induction machine. Substantial difference against the present article consists regarding the purpose of the technology: the authors assume its application in very small wind turbines, and adjust the methodology and solutions of specific problems accordingly.

Wind energy, as a renewable source, is the main topic of Singh and Kaur [4]. The authors describe a DFIG (doubly fed induction generator) connected to a FC. The performance of the system is analyzed through modeling a DFIG by solving state space equations in MATLAB/Simulink.

The available literature understands the simulation of FC and DFIM properties as a highly theoretical process supported by mathematical fundamentals. A typical example of a model with good mathematical background (emphasizing the different properties of brushless DFIM technology) can be found in Tohidy [5]. The author provides details of a static model as well as a dynamic model, and performs simulations in MATLAB/Simulink. However, unlike the present article, the primary criterion is the torque (torque characteristics) of the device. As for the problems that are closer to industrial applications, there are some partial and specific details, which are sometimes verified in laboratory conditions. For example, the starting method and DFIM speed control are analyzed in Yuan et al. [6]; transient stability improvement (for a grid-connected wind farm) is discussed and analyzed in Taj et al. [7].

Another area of interest is the spectral analysis of FC quantities, such as currents for example, but mainly voltages. Spectral analysis is an important element in the simulation, designing, and optimization of semiconductor devices. In the area of FC, it is based on the analysis of output quantities and their presentation in different two-dimensional (2D) or three-dimensional (3D) coordinate systems. Some problems are addressed, such as those regarding the cascade multilevel converter (Xu and Zou [8]), where the authors maximize the voltage density of a FC or confirm the theoretical fundamentals of analytical relationships connected with high-power multilevel voltage source converters in Jiang et al. [9].

Especially the research team of the Saint Petersburg Electrotechnical University (LETI) has been dealing with the problems regarding a FC for a DFIM. A variable speed drive for pump-storage application has been introduced in Pronin et al. [10], where a reversible turbine was powered by a DFIM. The multistage-multilevel converter has been implemented using this technology (Pronin et al. [11]).

The two papers focus on an in depth analysis of the mechanical and electrical properties of these technological systems. Here, the mathematical foundations for an important part of these systems were built. The calculations and simulations lead to the setting of electrical parameters for the interconnection and cooperation of individual elements within such a complex system (which includes power electronics, an electric machine, and a pumped-storage power plant in Pronin et al. [12]). The very principle of the new approach, i.e. the division of the main scheme into sub-circuits, is presented in Pronin et al. [13]. Here, the methodology is presented and tested on an example of a multistage-multilevel active FC. The calculation of the system parameters is discussed mainly in the dissertation thesis by Nahdi [14]. These works are followed by the analysis of a connection between a DFIM and a multistage-multilevel FC in Pronin et al. [1].

It follows from the above that a FC in conjunction with an induction machine is an important part of the present energy systems and technologies. This area introduces many partial problems depending on the required parameters, especially the transmitted power. These problems are analyzed and (successfully) solved by many authors. In general, it is possible to say that by increasing the efficiency of the equipment, the energy density is also increasing, as well as the demands for optimization of the available energy sources [10,11,14–17], with special emphasis on the use of semiconductor elements [18–24]. However, a comprehensive study that focuses on the issue of a FC with a given practical use, as presented in this article, has been lacking so far. Also, no comparison of the individual technologies has been available. The individual authors dealing with the given area have used their respective prescribed input parameters; as a result, mutual comparison of the results is very difficult, if not impossible. Therefore, this article is intended to provide such a study.

2. Modeling Methodology

Research on systems with DFIMs and FCs is based on the modeling of systems using the method of interconnected sub-systems. This approach allows creating computer models with a high-speed performance that is almost hundreds of times above that of models built in MATLAB in

Nahdi [14]. For the purpose of applying the systems modeling methodology on the interconnected sub-systems [12,14], a mathematical description of the FC (MMFC, for example, see Figure 1) has been developed. The MMFC contains a transformer with several three-phase secondary windings, a multistage active rectifier (AR) with several transistor bridges that are connected sequentially, capacitive filters of constant voltage with capacitors C_1-C_m , a multilevel inverter (VSI) for each branch, at which there are serially connected transistors, and reverse and separating diodes. An MMFC supply is based on a three-phase electric system characterized by its electromotive force with phases e_{sn} , inductances L_s , phase voltages U_{sn} , and currents i_{sn} ($n = 1, 2, 3$). The MMFC load is represented by an active resistance, R , inductance, L , and electromotive force, e_{gn} . U_n refers to the voltages of the loading phases, and I_n are the currents.

A control system (CS) is used for the stabilization of line voltages. The control system CS VSI is used for the regulation of the load currents, and the CS AR is used to control the rectifier. The division of the circuit in Figure 1 into sub-circuits consists of replacing the capacities represented by C_m by the dependent voltage sources represented by U_{cm} . The voltage sources represented by U_{cm} are connected to the branches of rectified currents of the detector bridges and of the inverter. Thus, the rectified currents of the detector bridges, i_{dm} , and the input currents of the inverter, i_{dim} ($m = 1, 5$), define the currents of the capacitors represented by i_{cm} , which can be further considered current sources. As a result of the specified conversions, the circuit in Figure 1 is divided into sub-circuits (Figure 2) that are conjunct by dependent sources of voltage U_{cm} and current i_{cm} . The conversion of a sub-circuit with detector bridges is implemented through the transformation of voltage sources U_{cm} into a circuit of rectified currents.

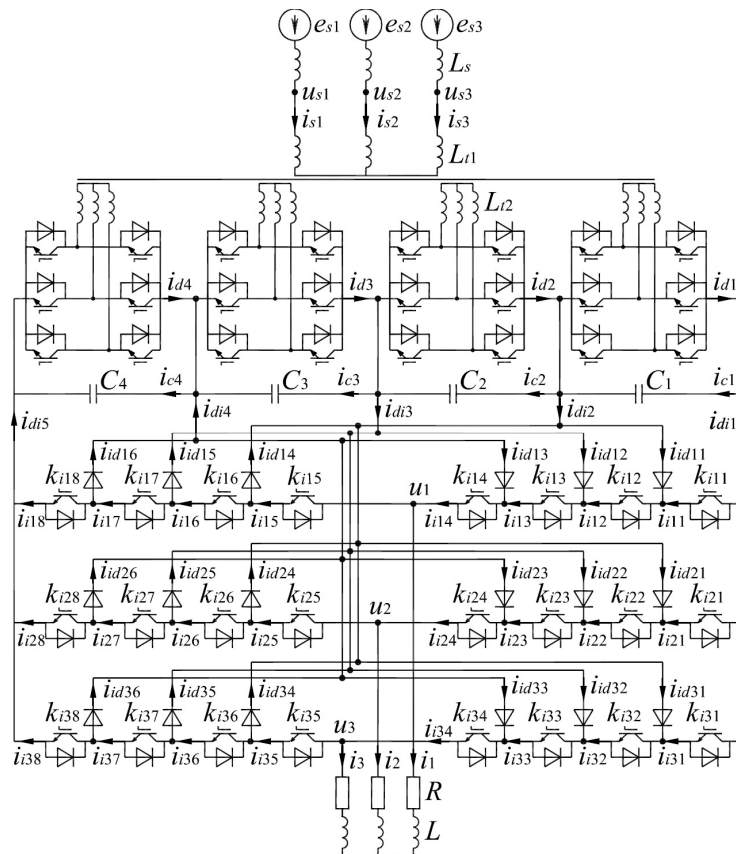


Figure 1. Mathematical description of the frequency converter (MMFC) scheme with a five-level multilevel inverter (VSI).

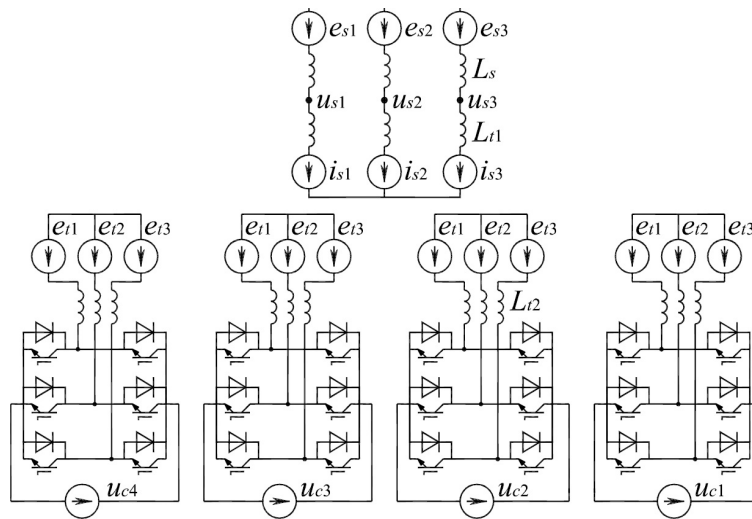


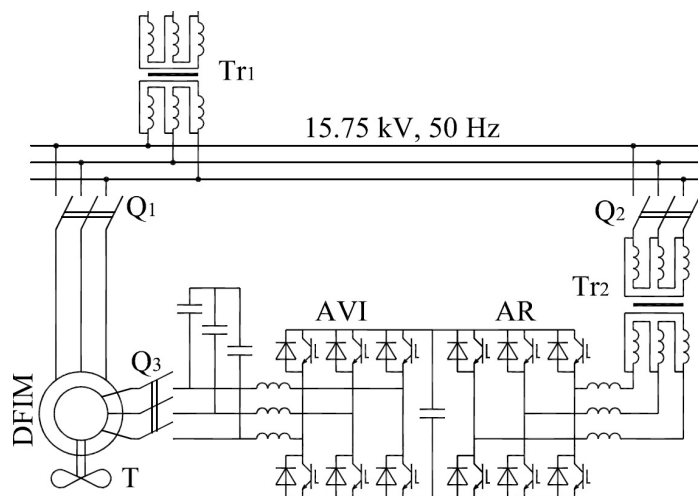
Figure 2. Conversion of the sub-circuit of an active rectifier (AR).

3. Two-Level Frequency Converter and an Asynchronous Generator Motor

The substantial improvement of the technical and economic indicators of pumped power station (PSS) is achieved by the use of semiconductor converters that are constructed on the basis of common elements (insulated-gate bipolar transistor—IGBT, Integrated gate-commutated thyristor—IGCT). The used exciting circuit of a DFIM, a transistor FC with two-level voltage inverters, can be seen in Scheme 1.

The two-level transistor FC contains a rectifier–inverter and an inverter–rectifier transistor (in the role of voltage converters). The two-level FC can transfer the electric power from the power network to the rotor of the DFIM, as well as in the opposite direction. The converter connected to the power network, which is maintaining the rectified voltage at the given level and providing sinusoidal currents of the network, ensures the operation in the power network with the given power factor. The converter connected to the rotor of the DFIM provides control of the rotor speed, voltage control, and control of the DFIM stator power factor.

In the scheme shown in Scheme 1, the transformer T_r sets the active power of the excitation system. In comparison with directly coupled thyristor FCs, the overall power of transformer T_r is roughly three times lower.



Scheme 1. Two-level frequency converter scheme.

Since the excitation system (Scheme 1) does not consume reactive power from the power network, compensating devices are not required. At the same time, rectifiers–inverters act as two-level converters of voltage, and considerably deform the voltage and the current at the input and the output of the FC.

Another difficulty is that at the high-rated power of the DFIM, the power of the two-level FC in the rotor circuit is also high. Thus, in the two-level FC, both serial and parallel inclusion of semiconductor devices or converting bridges is required [10,14]. Typical outputs of analysis can be seen in Figure 3.

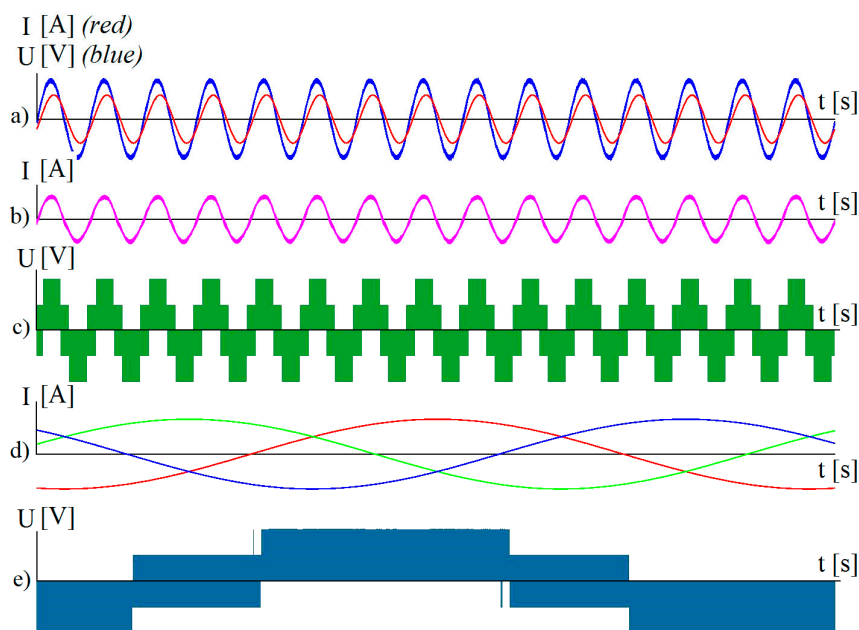


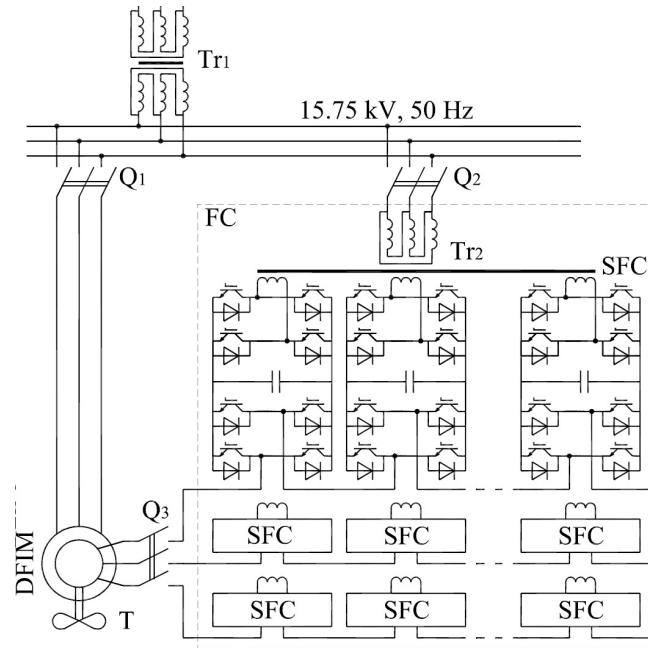
Figure 3. Typical example of voltage and current diagrams (two-level frequency converter): (a) network phase current (red), network phase voltage (blue); (b) active rectifier phase current; (c) active rectifier phase voltage; (d) inverter phase currents of a doubly fed induction machine (DFIM) rotor; (e) inverter phase voltage (DFIM rotor).

4. Three-Level Frequency Converter and an Asynchronous Generator Motor

The improvement in quality of the semiconductor converter and the complete system is achieved by replacing the two-level converter with a three-level one (Scheme 2). Dynamic losses of energy in the semiconductor elements are approximately two times lower than before. The peak-to-peak values of the voltage ripples at the input and at the output are also reduced two times. We can state that the three-level FC can be operated on twice as high voltage without the use of additional devices. However, at a high power of the DFIM, a three-level FC can appear insufficient when a somewhat higher voltage of the rotor of DFIM is required [12,14]. The current and voltage waveforms are shown in Figure 4.

A three-phase voltage control system is used to control the single-phase inverters. Inverter bridges are controlled by the specified control voltages. Thus, in the pulse width modulation mode, only one inverter operates in each phase of the load.

Subsequently, the dynamic losses of energy in the inverters are reduced, as well as the voltage ripples amplitude (proportionally to the quantity of serial connected bridges [10,14]). The current and voltage waveforms are shown in Figure 5.



Scheme 3. Cascade frequency converter scheme.

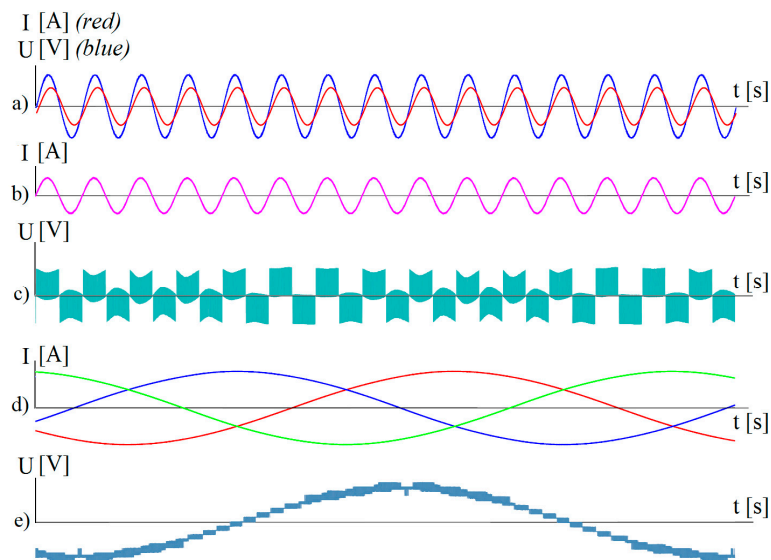
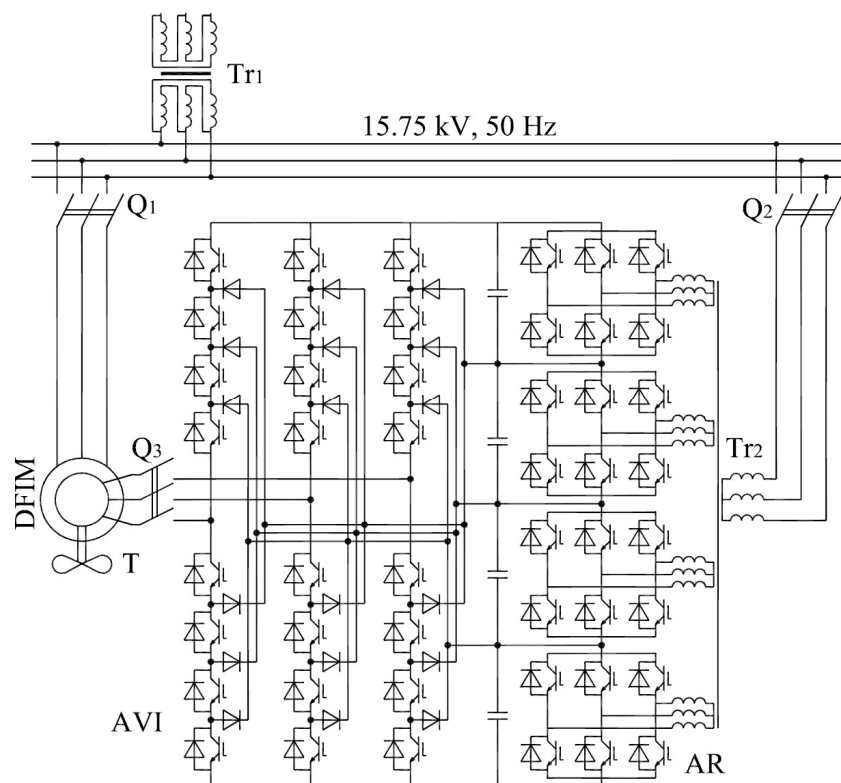


Figure 5. Typical example of voltage and current diagrams for a cascade frequency converter: (a) network phase current (red), network phase voltage (blue); (b) active rectifier phase current; (c) active rectifier phase voltage; (d) inverter phase currents (DFIM rotor); (e) inverter phase voltage (DFIM rotor).

6. Multistage-Multilevel Frequency Converter and an Asynchronous Generator-Motor

The MMFC (Scheme 4) consists of a medium voltage multistage pulse width modulation (PWM) rectifier, which is below referred to as an active rectifier (AR), and a multilevel inverter (VSI) with a neutral point diode-clamped topology. The AR is configured as a serial connection of four low-voltage IGBT bridges that are supplied from independent windings $w_{11}...w_{14}$ from a multi-wound step-down transformer. The DC-link voltage is formed as a sum of the output voltages from all of the bridges. The AR bridges are put into a multistage mode of operation through ensuring an appropriate phase shift between the triangular carrier signals that are taking part in the formation of pulses applied to the IGBT modules of adjacent bridges.

The above-presented system operates in a mode of multistage pulse width modulation. Each bridge of the AR has an individual CS. The MMFC enables the formation of a three-phase system of currents with a sinusoidal form in DFIM windings. Thus, the MMFC consumes sinusoidal currents (with a power factor close to 1) from the power network. It is necessary to state that the four secondary circuits of the transformer are loaded non-uniformly. In the first and fourth secondary circuit, sudden changes of current amplitude are observed. Therefore, if the value of rated power is based on the most loaded windings, the sizes of the transformers are obviously enlarged. Nevertheless, secondary circuits can be loaded with a variable power. Despite these facts, the dimensions and costs of the equipment can be reduced [11,13,14]. The current and voltage waveforms are shown in Figure 6.



Scheme 4. Multistage-multilevel frequency converter scheme.

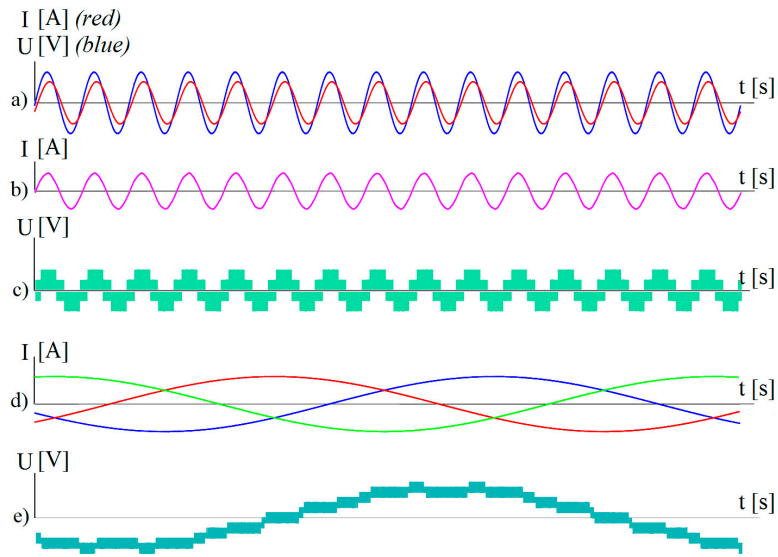


Figure 6. Example of voltage and current diagrams for a multistage-multilevel frequency converter: (a) network phase current (red), network phase voltage (blue); (b) active rectifier phase current; (c) active rectifier phase voltage; (d) inverter phase currents (DFIM rotor); (e) inverter phase voltage (DFIM rotor).

7. Spectral Analysis of the Output Voltage of the Used Frequency Converters

It is clear that the FC creates higher harmonics on the rotor winding. Higher harmonics cause additional losses of energy and vibrations in electrical machines. The above-mentioned overloads adversely affect the insulation. The presence of higher harmonics in the circuit of rotor requires additional research (Nahdi [14]).

Spectrograms of the output voltage can be seen in Figures 7–10. The data are based on the pulse width modulation frequency $f_{PWM} = 4 \text{ kHz}$, and control frequency $f_C = 3.57 \text{ Hz}$.

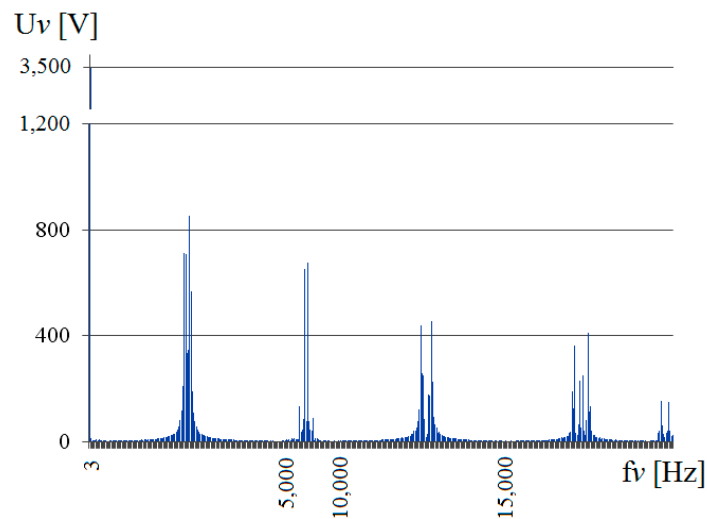


Figure 7. Output voltage spectrogram: two-level frequency converter.

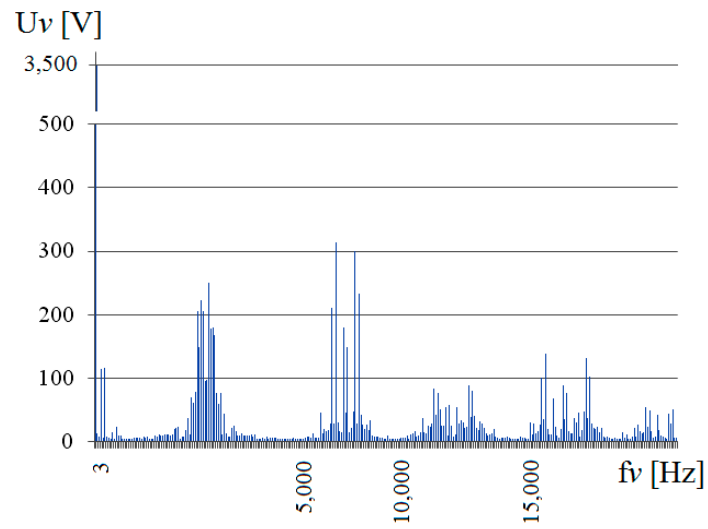


Figure 8. Output voltage spectrogram: three-level frequency converter.

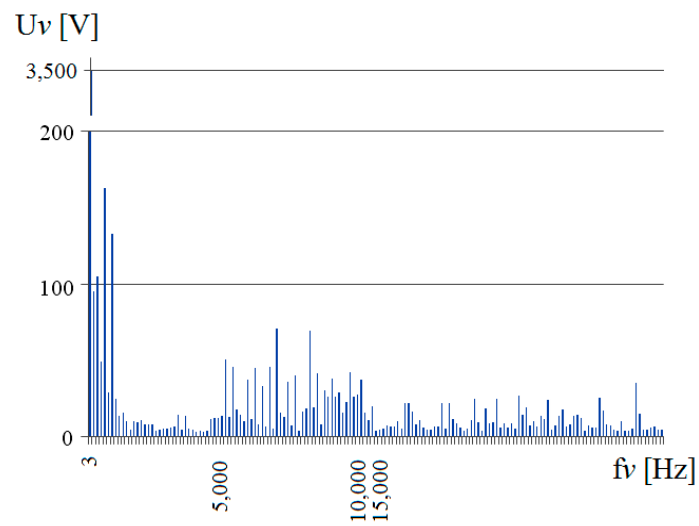


Figure 9. Output voltage spectrogram: cascade frequency converter.

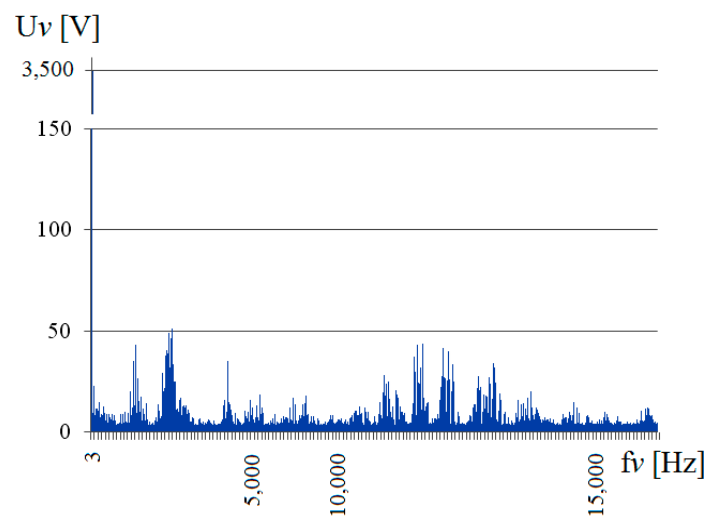


Figure 10. Output voltage spectrogram: multistage-multilevel frequency converter.

The dependence of the voltage distortion factor K_v on the type of the FC (at $f_{PWM} = 4$ kHz) can be seen in Figure 11. The best results, from this point of view, are obtained using a cascade FC.

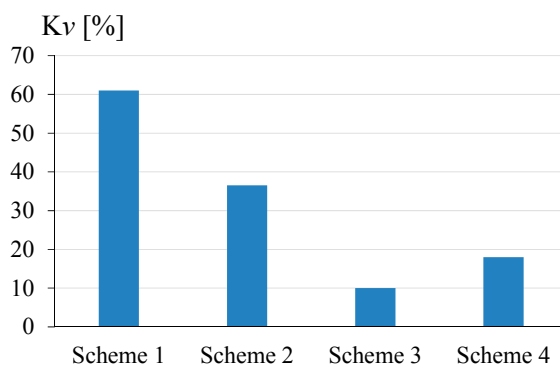


Figure 11. Voltage distortion factor K_v .

8. Comparative Analysis of the Used Frequency Converters

Comparative analysis has been done based on computer models developed through the collaboration between Dr. Nahdi and the Power Machines company (Nahdi [14]). All of the calculations were performed for the motoring operation mode of a DFIM with the following parameters (the values are precisely mapping the parameters of the prototype deployed in the Power Machines company):

Active power of DFIM $P = 274$ MW, $\cos\varphi = 0.95$, stator winding voltage $U = 15.75$ kV, frequency $f = 50$ Hz, reduction factor of the rotor winding parameters equal to five, leakage inductance of the stator phase $L_{s1} = 0.18$ pu (a fraction of the base unit quantity, pu), leakage inductance of the rotor phase $L_{s2} = 0.173$ pu, magnetizing inductance $L_m = 1.79$ pu, active resistance of the stator phase 0.0016 pu, active resistance of the rotor phase 0.029 pu, moment of resistance on the shaft at the start-up 7%.

Calculations have been performed for rotor slip $s = -0.07142857$, which corresponds to the rotor speed $n = 1.07142857$ pu. At the specified slip, the major part of the active power (92.9%) flows from the power supply system to the turbine shaft through the winding of the stator and the air gap of the DFIM. A smaller part of the power (7.1428%) is transferred from the power supply system to the turbine shaft through the FCs and the DFIM rotor winding. In this mode, the DFIM rotor current frequency ($f_r = 3.57$ Hz) is proportional to the frequency of the power supply system ($f_s = 50$ Hz) and the slip. It allows obtaining a periodic response and reducing the errors of calculations at the analysis of currents and voltages (Figures 3–6).

It is necessary to extract the parameter of “power imbalance” from the results. Ideally, it should be equal to 0 (in the steady-state operating mode of the system), which follows the energy conservation laws. However, in the calculations, it differs from 0, and this difference characterizes the accuracy of the calculations caused by the restriction in quantity of the iterations, errors of integration, round-off errors, the level of harmonics analysis, etc. In the considered cases, the errors of calculations do not exceed 0.43% (see Table 1).

In the considered calculations, the control algorithm provides approximately the same operating mode of the system (slip of DFIM, active and reactive powers of the power supply and DFIM, modulation factor of the rectifiers and inverters, etc.).

It is necessary to mention the difference between the total rotor power and the power at the basic harmonic. The total power of the rotor is the highest (26.05 MW) for Scheme 1 (Table 1). This is due to considerable voltage distortion at the output of the FC (Figure 3). In Scheme 2, the voltage of the rotor is deformed less (Figure 4), and the total power of the rotor is reduced to 21.87 MW. The best forms of the voltage of the rotor are obtained for Schemes 3 and 4. In these systems, the total rotor power is minimal, and it also comes closer to the total power at the basic harmonic (20.5 MVAR).

Table 1. Frequency converter systems characteristics.

Parameters of PSS with DFIM and FC in the Circuit of Rotor	Scheme 1 Two-Level FC	Scheme 2 Three-Level FC	Scheme 3 CASCADE FC	Scheme 4 MMFC
Frequency of pulse-width modulation f_{PWM} [Hz]	4000	4000	4000	4000
Rotor speed of DFIM [pu]	1.0712	1.0742	1.0742	1.0742
Active power of the power system [MW]	273.93	273.93	273.91	273.93
Reactive power of the power system [MVAR]	96.5	96.5	96.5	96.5
Active power of the stator [MW]	255.32	254.91	255.62	255.85
Reactive power of the stator [MVAR]	97.06	97.93	96.27	96.75
Active power in the DFIM rotor circuit [MW]	18.61	19.02	18.3	18.09
Shaft power of DFIM [MW]	272.33	271.77	272.67	272.87
Total power of the rotor of DFIM [MW]	26.05	21.87	20.58	20.82
Total power of DFIM rotor at the first harmonic [MW]	20.55	20.4	20.47	20.52
Power of the transformer primary windings [MW]	18.82	19.06	18.31	18.09
Power of the transformer secondary windings [MW]	22.91	19.82	25.52	32.19
Power of the rectifiers keys [MW]	173.7	173.2	454	180
Power of the inverters keys [MW]	179.9	179.7	176.9	180
Power of the isolating diodes [MW]	-	167	-	135
Energy of capacities ($0.5 \sum CU^2$) [kJ]	500	500	1,500	500
Network voltage distortion factor [%]	3.98	3.57	2.76	0.34
Network current distortion factor [%]	0.44	0.34	0.819	0.13
Rotor voltage distortion factor [%]	61	36	10.4	17
Rotor current distortion factor [%]	0.18	0.29	1.0	0.053
Rectifiers modulation factor amplitude	0.819	0.809	0.818	0.825
Inverters modulation factor amplitude	0.818	0.809	0.815	0.791
Rectified voltage [V]	10,000	10,000	820	10,000
Rotor phase voltage at the first harmonic [V]	3236	3218	3224	3224
Rectifier phase effective current [A]	1859	1900	3237	2639
Inverter phase effective current [A]	2117	2113	2116	2121
Rotor phase effective current [A]	2117	2113	2116	2121
Power imbalance	0.25	0.43	0.13	0.06

In the considered schemes, the active rectifiers, maintaining the given rectified voltage, provide sinusoidal currents of the transformer, and operate with a power factor of the transformer close to 1. Due to small deformations of the voltages and currents at the transformers' primary windings, their total outputs are roughly the same in different schemes (18.82; 19.06, 18.31; 18.09 MW). The total powers of the transformers' secondary windings in the schemes differ significantly. For a three-level FC, the voltage rectifier distortion is the smallest, and the overall secondary winding power of the transformer is minimal (19.82 MW). For a cascade FC (Scheme 2), the distortions of the rectified voltage are higher, and the total power of the secondary winding of the transformer above is 25.52 MW. In this scheme, the secondary winding power is also increased, since sudden changes of current amplitude are observed here (Pronin et al. [11]).

In Scheme 4, sudden changes of current amplitude in the transformer appear, and the rectifier bridges are loaded non-uniformly. The highest total power of transformer secondary windings (defined on the most loaded winding) is 32.19 MVAR. However, if the transformers' secondary windings are loaded with varying power (in this case two times 8.05 MVAR, and two times 3.9 MVAR), the total capacity of secondary windings decreases to 23.9 MVAR.

To be able to compare the considered schemes for the performance of the semiconductor key elements, it is necessary to define the critical performance indicator. It can be described as a multiplication of the current amplitude in the key element, the voltage amplitude, and the quantity of the same key elements operating in identical conditions. This indicator shows the best features of a two-stage FC (Scheme 1). For a three-level FC (Scheme 2), the total power of the semiconductor devices is almost 1.5 times higher, which is caused by the used diode modules. The total power of the semiconductor devices for a cascade FC is 1.8 times higher than that in Scheme 1 due to the use of single-phase bridges, and also to the non-uniformity of the load. The results for Scheme 4 are close to those for Scheme 2.

The capacities of the FC capacitors, as well as the rectified voltage, were chosen with the aim of stabilizing the steady and transient electromechanical processes. Thus, in Scheme 1, a capacitor with capacity of 10,000 μF (at 10,000 V) is used, resp. 20,000 μF (5000 V, Scheme 2), 250,000 μF (820 V, Scheme 3), and 40,000 μF (2,500 V, Scheme 4).

Following the local standard GOST 13109-07 for electrical systems with voltages between 6–20 kV, the voltage distortion factor should not exceed 5%. The obtained voltage distortions always have smaller levels for all of the considered schemes. Using this criterion, the scheme with a cascade FC (Table 1, Scheme 3) provides the best results.

However, the frequency inverters deform the DFIM rotor voltage. The distortion factor reaches 61% in the scheme with a two-level FC, 36% in the scheme with a three-level FC, and 10% in the scheme with a cascade FC. In the scheme with a multistage-multilevel FC, the distortion factor reaches 17%. However, it is necessary to consider that the FC can be loaded on a larger number of levels, and this factor can be significantly reduced.

When comparing PSS schemes, it is also necessary to consider some practical possibilities of the FC's construction. The use of high-speed modules IGBT calculated for relatively low voltages is possible for Schemes 3 and 4. Thus, it is possible to ensure the operation of the FCs in the mode of pulse width modulation at a frequency of the reference voltage (e.g., 4000 Hz). Schemes 1 and 2 can also be realized using low-frequency semiconductor devices with low-frequency pulse width modulation. Taking into account the set of criteria (semiconductor devices power, capacitors energy storage, input/output voltages, and current distortions), Scheme 4 should be the best solution.

Differences of the most important characteristics for the respective schemes are even more noticeable in the graphical presentation of values provided in Table 1. A clear comparison of powers in the system (the total power of the rotor, power of the transformer primary and secondary windings and power of the rectifiers keys) can be seen in Figure 12. Comparison of the distortion factors is shown in Figure 13 while the rectifier currents are visualized in Figure 14.

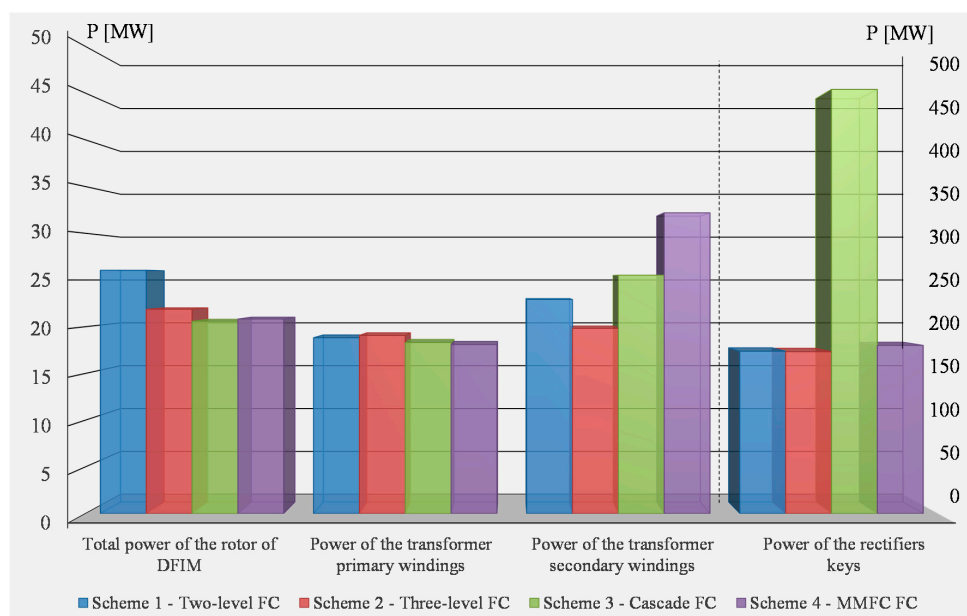


Figure 12. Graphical comparison of power in the system: (1) total power of DFIM (scale on the left); (2) power of transformer primary windings (scale on the left); (3) power of the transformer secondary windings (scale on the left); (4) power of the rectifiers keys (scale on the right).

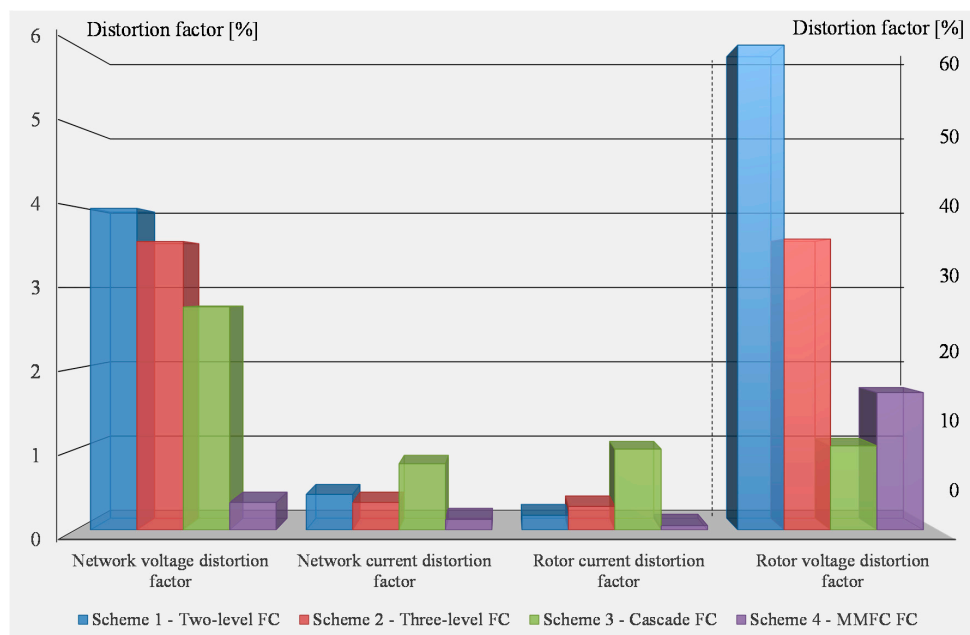


Figure 13. Graphical comparison of distortion factor: (1) network voltage distortion factor (scale on the left); (3) network current distortion factor (scale on the left); (2) rotor current distortion factor (scale on the left); (4) rotor voltage distortion factor (scale on the right).

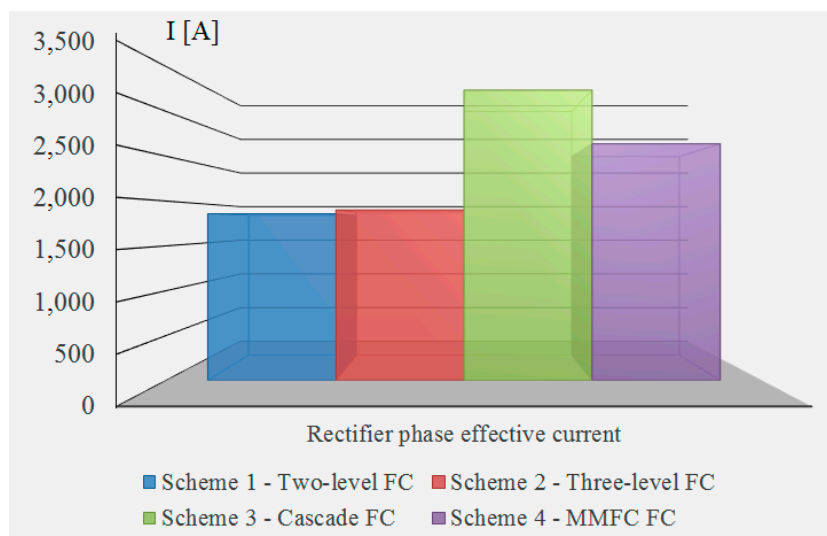


Figure 14. Comparison of rectifier effective currents.

9. Discussion and Practical Consequences of the Results

The developed structure of power electronic systems with a DFIM and different types of FCs, models, results of research, and recommendations can be used for designing new mechatronic systems with DFIMs and various kinds of FCs. The developed computer models precisely describe the objects of the research, and they are fast, which ensures their efficiency in calculations and studies of the transient and steady modes. The offered techniques for defining high-frequency parameters of machines and the estimation of additional losses can be used for the specification of technical solutions in designing systems with DFIMs. The reliability of the models and results is confirmed by the successful use of the methodology by electric machine producers, and also by the training process at the Saint Petersburg Electrotechnical University (LETI).

10. Conclusions

The article provided a comprehensive view of the properties and behavior of FC–DFIM systems. The analyzed systems serve as electrical equipment for a pumped-storage power plant. The priority of this analysis was the designing of an original mathematical model of the FC based on the interconnected sub-systems presented herein. Another important step was the calculation of the essential operating parameters of these systems. From these procedures, the authors came to the following conclusions:

- The article presents models of four FC topologies connected to a DFIM, namely: a two-level, three-level, cascade, and multistage-multilevel FC.
- The presented modeling methodology based on interconnected sub-systems leads to rapid responses of the computer system, and thus also to more efficient use of central processing unit (CPU) time.
- In all of the considered variants of FCs that are considering higher harmonics in a broad spectrum, the supply voltage distortion factor of the rotor of the DFIM exceeds 10%. This demonstrates the need to analyze and take into account the effect of higher harmonics on electromagnetic processes in the PSS, DFIM energy losses, and the reliability of the system.
- A comparative analysis of PSS schemes with a doubly fed induction machine, and FCs of various types in the rotor circuit has been made.
- Taking into account the set of indicators, such as the power of semiconductor devices, capacitors energy storage, input/output voltages and currents, the use of IGBT high-speed modules etc., it is recommended to use a PSS scheme with a multistage FC in the DFIM rotor circuit.
- On the basis of complex evaluation of the parameters, the multistage FC has the most favorable values for:
 - A network voltage distortion factor (9% compared to the maximum value achieved for another converter scheme);
 - rotor current distortion factor (5% compared to the maximum value achieved for another converter scheme);
 - power imbalance (14% compared to the maximum value achieved for another converter scheme);
 - the total power of the rotor is minimal here (together with Scheme 3, the cascade FC) while maintaining the rotor speed, the active and reactive power of the power system, the active power of the stator, and the total power of the DFIM rotor at the first harmonic.

The above assessment contributes to a significant improvement in the efficient use of the available energy during the operation of the described system.

Acknowledgments: The research has been supported by an internal grant of the Faculty of Electrical Engineering, CTU in Prague.

Author Contributions: Tarek Nahdi designed the technologies and the experiments, performed the experiments/computer simulations; Dusan Maga analyzed the data, overviewed on state-of-the-art and wrote the paper.

Conflicts of Interest: The authors declare no conflict of interest. The founding sponsors had no role in the design of the study; in the collection, analyses, or interpretation of data; in the writing of the manuscript, and in the decision to publish the results.

References

1. Pronin, M.; Shonin, O.; Vorontsov, A.; Gogolev, G. Features of a Drive System for Pump-storage Plant Applications based on the Use of Double-fed Induction Machine with a Multistage-multilevel Frequency Converter. In Proceedings of the 2012 15th European Conference on Power Electronics and Applications, Novi Sad, Serbia, 4–6 September 2012.
2. Steimer, P.K.; Senturk, O.; Aubert, S.; Linder, S. Converter-fed Synchronous Machine for Pumped Hydro Storage Plants. In Proceeding of the 2014 IEEE Energy Conversion Congress and Exposition (ECCE), Pittsburgh, PA, USA, 14–18 September 2014; pp. 4561–4567.
3. Cuesta, A.B.; Gomez-Gil, F.J.; Fraile, J.V.M.; Rodríguez, J.A.; Calvo, J.R.; Vara, J.P. Feasibility of a Simple Small Wind Turbine with Variable-Speed Regulation Made of Commercial Components. *Energies* **2013**, *6*, 3373–3391. [[CrossRef](#)]
4. Singh, P.; Kaur, A. Power Control of Doubly Fed Induction Generator (DFIG) Using Back To Back Converters (PWM Technique). In Proceedings of the 2014 IEEE International Conference on Advanced Communication Control and Computing Technologies (ICACCCT), Ramanathapuram, India, 8–10 May 2014.
5. Tohid, S. Analysis and Simplified Modelling of Brushless Doubly-fed Induction Machine in Synchronous Mode of Operation. *IET Electr. Power Appl.* **2016**, *10*, 110–116. [[CrossRef](#)]
6. Yuan, X.; Chai, J.; Li, Y. A Converter-Based Starting Method and Speed Control of Doubly Fed Induction Machine with Centrifugal Loads. *IEEE Trans. Ind. Appl.* **2011**, *47*, 1409–1418. [[CrossRef](#)]
7. Taj, T.A.; Hasanien, H.M.; Alolah, A.I.; Muyeen, S.M. Transient Stability Improvement of a Grid-connected Wind Farm Using Doubly Fed Induction Machine Based Flywheel Energy Storage System. In Proceedings of the Power and Energy Engineering Conference (APPEEC), Hong Kong, China, 7–10 December 2014.
8. Xu, Y.; Zou, Y. Spectral Analysis of an Improved Hybrid Cascade Multilevel Converter. In Proceedings of the 6th International Power Electronics and Motion Control Conference, Wuhan, China, 17–20 May 2009.
9. Jiang, X.; Xiao, X.; Liu, H.; Ma, Y. The Output Spectrum Analysis of High-Power Multilevel Voltage Source Converters using Double Fourier Series. In Proceedings of the 2005 IEEE/PES Transmission & Distribution Conference & Exposition, Dalian, China, 14–18 August 2005.
10. Pronin, M.; Shonin, O.; Vorontsov, A.; Gogolev, G. A Pumped Storage Power Plant with Double-Fed Induction Machine and Cascaded Frequency Converter. In Proceedings of the 2011 14th European Conference on Power Electronics and Applications, EPE 2011, Birmingham, UK, 30 August–1 September 2011.
11. Pronin, M.; Shonin, O.; Gogolev, G.; Vorontsov, A.; Nahdi, T. A Double-fed Induction Machines with a Multistage-multilevel Frequency Converter for Pumped Storage Power Plant Applications. In Proceedings of the 2011 IEEE Power Engineering and Automation Conference, PEAM 2011, Wuhan, China, 8–9 September 2011; pp. 221–225.
12. Pronin, M.; Vorontsov, A.; Nahdi, T.; Kouzin, M. Analysis of Operating Modes of Asynchronised Machines for Pumped-storage Power Plants. *Proc. IEEE Russ. North West Sect.* **2011**, *1*, 51–53.
13. Pronin, M.; Vorontsov, A.; Nahdi, T.; Kouzin, M. Modelling of the Multistage-multilevel Active Frequency Converter by a Method of the Interconnected Subcircuits. *Proc. IEEE Russ. North West Sect.* **2011**, *2*, 35–38.
14. Nahdi, T. Modeling and Designing of Systems with Induction Machines and Active Multilevel Frequency Converters. Ph.D. Thesis, Saint Petersburg Electrotechnical University “LETI”, Saint Petersburg, Russia, 2012.
15. Janning, J.; Schwery, A. Next Generation Variable Speed Pump-storage Power Stations. In Proceedings of the 2009 13th European Conference on Power Electronics and Applications, EPE'09, Barcelona, Spain, 8–10 September 2009.
16. Bocquel, A.; Janning, J. Analysis of a 300 MW Variable Speed Drive for Pump-storage Plant Applications. In Proceedings of the 2005 European Conference on Power Electronics and Applications, Dresden, Germany, 11–14 September 2005.
17. Bocquel, A.; Janning, J. 4 × 300 MW Variable Speed Drive for Pump-Storage Plant Application. In Proceedings of the European Conference on Power Electronics and Applications, Toulouse, France, 2–4 September 2003.
18. Zhou, Y.; Bauer, P.; Ferreira, P. Operation of Grid-Connected DFIG under Unbalanced Grid Voltage Condition. *IEEE Trans. Energy Convers.* **2009**, *24*, 240–246. [[CrossRef](#)]

19. Bauer, P.; Schoevaars, R. Bidirectional Switch for a Solid State Tap Changer. In Proceedings of the 2003 IEEE 34th Annual Power Electronics Specialists Conference, Acapulco, NM, USA, 15–19 June 2003; pp. 466–471.
20. Rosen, M.A.; Nicola, D.A.; Bulucea, C.A.; Cismaru, D.C. Sustainability Aspects of Energy Conversion in Modern High-speed Trains with Traction Induction Motors. *Sustainability* **2015**, *7*, 3441–3459. [[CrossRef](#)]
21. Skvortsov, B.; Nahdi, T.; Maga, D. Mechatronic System with a Turbo-generator of two Different Frequencies. In Proceedings of the 12th International Conference on Mechatronics, Brno, Czech Republic, 6–8 September 2017; pp. 302–310.
22. De Jong, E.C.W.; Ferreira, J.A.; Bauer, P. Design Techniques for Thermal Management in Switch Mode Converters. *IEEE Trans. Ind. Appl.* **2006**, *42*, 1375–1386. [[CrossRef](#)]
23. Helle, L.; Munk-Nielsen, S. Comparison of Converter Efficiency in Large Variable Speed Wind Turbines. In Proceedings of the 16th Annual IEEE Applied Power Electronics Conference and Exposition, Anaheim, CA, USA, 4–8 March 2001; pp. 628–634.
24. Holmes, D.G.; Lipo, T.A. *Pulse Width Modulation for Power Converters. Principles and Practice*; Wiley Press: Hoboken, NJ, USA, 2003; ISBN 978-0-471-20814-3.
25. Skvorcov, B.A.; Baygildina, E.I. Cascade Matrix Converter. *Proc. IEEE Russ. North West Sect.* **2011**, *1*, 33–39.



© 2018 by the authors. Licensee MDPI, Basel, Switzerland. This article is an open access article distributed under the terms and conditions of the Creative Commons Attribution (CC BY) license (<http://creativecommons.org/licenses/by/4.0/>).